A fluorescence biosensor for VEGF detection based on DNA assembly structure switching and isothermal amplification

Junlong Li, Kexin Sun, Zhongping Chen, Jifei Shi, Dandan Zhou, Guoming Xie

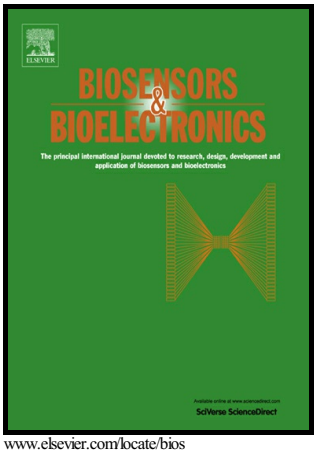

www.elsevier.com/locate/bios

PII: S0956-5663(16)30963-0
DOI: http://dx.doi.org/10.1016/j.bios.2016.09.078
Reference: BIOS9190

To appear in: *Biosensors and Bioelectronic*

Received date: 2 August 2016
Revised date: 19 September 2016
Accepted date: 22 September 2016

Cite this article as: Junlong Li, Kexin Sun, Zhongping Chen, Jifei Shi, Danda Zhou and Guoming Xie, A fluorescence biosensor for VEGF detection based o DNA assembly structure switching and isothermal amplification, *Biosensors an Bioelectronic,* http://dx.doi.org/10.1016/j.bios.2016.09.078

Title: A fluorescence biosensor for VEGF detection based on DNA assembly structure switching and isothermal amplification

Junlong Li[a], Kexin Sun[a], Zhongping Chen[b], Jifei Shi[c], Dandan Zhou[d], Guoming Xie[a*]

[a]Key Laboratory of Laboratory Medical Diagnostics, Ministry of Education, Department of Laboratory Medicine, Chongqing Medical University, Chongqing 400016, PR China

[b]Department of Clinical Laboratory, Chongqing Municipal Jiulongpo District the First People's Hospital, Chongqing 400050, PR China

[c]Institute of Medical Technology, Baotou Medical College, Baotou 014060, PR China

[d]Clinical Laboratory, The First Affiliated Hospital, Chongqing Medical University, Chongqing 400016, PR China

guomingxie@cqmu.edu.cn

xiegm059@foxmail.com

[*]Correspondence author: Key Laboratory of Laboratory Medical Diagnostics of Education, Ministry of Education, Department of Laboratory Medicine, Chongqing Medical University, No. 1 Yi Xue Yuan Road, Chongqing 400016, PR China, Tel.: +86 23 68485240; fax: +86 23 68485240

Abstract

Vascular endothelial growth factor (VEGF) is an important biomarker in cancer angiogenesis. Here, we develop a aptasensor method for VEGF detection based on DNA assembly structure switching and isothermal amplification. The design employs a DNA assembly made of a isothermal amplification template, a aptamer, a primer and a protector chain. The DNA assembly is unable to undergo isothermal amplification in the absence of target. The presence of the target, however, triggers a structure switching event that causes hybridization of primer with template to facilitate isothermal amplification. Whereafter, toehold-mediated DNA strand displacement reaction between the generated (single-stranded DNA) ssDNA and fluorescent/quencher labeled probe are performed. Then, the increase in fluorescence provides an analytical signal. This strategy opens up a sensitive, selective and simple sensing platform for detection of VEGF. The system was also implemented to analyze the VEGF in human serum samples with satisfactory results.

Keywords: Vascular endothelial growth factor (VEGF); Aptamer; Fluorescence biosensor; Isothermal amplification

1. Introduction

Vascular endothelial growth factor (VEGF), primevally known as vascular permeability factor (VPF) (Senger et al., 1983), plays central roles in the regulation of angiogenesis and vascular permeabilization (Leung et al., 1989). VEGF is a part of the system that restores the oxygen supply to tissues when blood circulation is inadequate (Prior et al., 2006). Over expression of VEGF can cause vascular disease in the retina of the eye and other parts of the body (Gupta et al., 2013; Park et al., 2014; Do et al., 2016). Serum concentration of VEGF is high in bronchial asthma (Tsai et al., 2015) and diabetes mellitus (Domigan et al., 2015). Solid cancers can not grow beyond a limited size without an adequate blood supply; cancers that can express VEGF are able to grow and metastasize (Belcik et al., 2012; Urquidi et al., 2012). Therefore, serum level of VEGF has significant implications as biomarker for some diseases and subsequent monitoring of treatment. The VEGF family comprises five members including VEGF-A, VEGF-B, VEGF-C, VEGF-D and placenta growth factor (PGF) (Wei et al., 2013). Several components of the VEGF family have different spliced forms that vary in their angiogenic effects. Such as, human VEGF-A has at least 6 isoforms: 121, 145, 165, 183, 189, and 206 (Abdel-Rahman, 2015; Marone et al., 2016). $VEGF_{165}$ is the most potent pro-angiogenic isoforms and is commonly overexpressed in a variety of human tumors (Niu and Chen,

2010; Nonaka et al., 2013). Therefore, $VEGF_{165}$ is selected as the target protein in this work.

Traditional technique for VEGF detection in clinical is enzyme linked immunosorbent assays (ELISA) (Goncalves et al., 2007; Rifai et al., 2006; Takahashi et al., 2016). However, the antibody-based method require large sample volume and expensive reagents. Furthermore, ELISA is labor intensive and require long incubation times. The ability to select nucleic acids (aptamers) with specific recognition properties toward proteins introduced new opportunities to VEGF detection (Nonaka et al., 2010). Aptamers have high affinity, specificity, and stability; therefore, they are regarded as alternative reagents to antibodies (Potyrailo et al., 2015; Lee et al., 2015; Li et al., 2015; Liu et al., 2015). To date, a number of aptamer-based VEGF detection techniques have been developed (Freeman et al., 2012; Cho et al., 2012; Wang and Si, 2013; Chen et al., 2014; Kirsch et al., 2013; Li et al., 2015b; Zhang et al., 2015; Wimmer et al., 2016). While, the relationship between aptamer and target is one-to-one correspondence in almost all of the technologies. Thus, they lack of signal amplification strategy, resulting in low sensitivity and high error rate. Though some analytical platforms that analyzed VEGF sensitively were reported (Kwon et al., 2010; Kwon et al., 2012; Zhao et al., 2015a), but the detection range of these methods is narrow, can't meet the demand of clinical actual test. For these reasons, a simple

amplification method with wide detection range is in strong demand for VEGF detection.

Herein, we present a new aptamer-based VEGF detection fluorometric method. Compared with electrochemistry and SPR, fluorescence approaches do not exist interfacial effect (Xue et al., 2011). Meanwhile, the sensitivity of fluorescence is better than that of colorimetry. On account of these, fluorescence technology has outstanding performance in biosensing new method developments (Gao et al., 2015; Guo et al., 2015; Jeong et al., 2015). An enzymatic isothermal amplification for short oligonucleotides was devised in 2003 (Van Ness et al., 2003). It's an amplification technique that combines polymerase strand extension with single-strand nicking (Nie et al., 2015; Zhao et al., 2015b; Li et al., 2016). The reaction provides 10^6 - 10^9 fold amplification under isothermal conditions. Compared with other amplification methods, the EXPAR method has the distinct advantages of its isothermal nature, high amplification efficiency, and rapid amplification kinetics. In this technique, we introduced this amplification mechanism. A DNA assembly is forming by four DNA nucleic acids at first. In the presence of the target, it induces the structural modification of the DNA assembly and triggers isothermal amplification reaction to produce single-stranded DNA (ssDNA). The 5 nt unhybridized region of the fluorescent/quencher labeled probe serves as a

toehold for complementary ssDNA, and the increase in fluorescent material provides an analytical signal. Thus, this technology has great potential for the development of an effective detection method for VEGF.

2. Experimental

2.1. Reagents and materials

All oligonucleotide sequences were synthesized and purchased from Sangon Biotechnology Co. (Shanghai, China), and the oligonucleotide sequences were provided in Table S1. Bst DNA polymerase (large fragment), Nb.BbvCI nicking enzyme and ThermoPol buffer (10×) were purchased from New England Biolabs, Inc. (Beverly, MA, USA). Goodview nucleicTM acid stain (HGV-Ⅱ) was purchased from SBS Genetech Co., Ltd. (Beijing, China). Deoxynucleotide triphosphates (dNTPs) were obtained from Thermo Fisher Scientific (Massachusetts, USA). Premix Taq™ (TaKaRa Taq™ Version 2.0 plus dye), 20 bp DNA Ladder and loading buffer (6×) were purchased from TaKaRa Biotechnology Co. Ltd. (Dalian, China). Acryl/Bis solution (29: 1), 30% (w/v) was purchased from Sangon Biotechnology Co. (Shanghai, China). Ammonium persulfate (APS) and Tetramethylethylenediamine (TMEDA) were purchased from Sigma-Aldrich (St.Louis, USA). Diagnostic Kit for Vascular endothelial growth factor (ELISA) was purchased from Bjjpjx

(Beijing, China). Ultrapure water (Milli-Q18.2 MΩ, Millipore System Inc.) was used for all the experiments.

2.2. Instrumentations

Fluorescence signals were recorded using a Cary Eclipse Fluorescence spectrophotometer (Agilent, California). Electrophoresis apparatus (DYY-6C, LIUYI, China) was used in electrophoresis experiment. Gel image was recorded on an imaging system (Bio-Rad Laboratories, USA).

2.3. Fluorescence detection

Parameters of scan: Scanning intervals, 1 nm; scanning speed, 600 nm/min; Excitation slit, 5 nm; Emission slit, 10 nm; Excitation wavelength, 480 nm; Emission wavelength, 500 nm-650 nm.

Parameters of kinetics: Scanning intervals, 2 min (samples detection) and 5 min (the optimal reaction temperature exploration); Excitation slit, 5 nm; Emission slit, 10 nm; Excitation wavelength, 480 nm; Emission wavelength, 520 nm.

2.4. Isothermal amplification system

The system in 60 μL contained 5 nM DNA (1)(2)(3)(4), 200 nM DNA (5)(6), 4×10^{-4} M dNTPs, 1.6 U Bst DNA polymerase (large fragment), 10

U Nb.BbvCI nicking enzyme, 1× ThermoPol buffer (20 mM Tris-HCl, 10 mM KCl, 10 mM $(NH_4)_2SO_4$, 2 mM $MgSO_4$, 0.1% Triton X-100, pH 8.8 @ 25 °C). The reaction was initiated by adding different concentrations of target and incubated at 37 °C.

2.5. Gel electrophoresis

The 8% native polyacrylamide gel was freshly prepared at laboratory, and native-PAGE (polyacrylamide gel electrophoresis) was carried out at a constant voltage at 120V for 50 min. The dye was HGV-Ⅱ nucleic acid dye staining. Electrophoresis apparatus (DYY-6C, LIUYI, China) was used for the electrophoresis experiments. At last, the gels were photographed by Bio-RAD digital imaging system.

2.6. Enzyme-linked immunosorbent assay

1: 1 diluted human serum samples were assayed for $VEGF_{165}$ using an ELISA kit according to the manufacturer's instructions. Firstly, 200 μL samples were added into the holes and incubated for 60 min at 37 °C, followed by a thorough washing with washing buffer. Secondly, 200 μL enzyme labeled reagent were added in the holes and incubated for 60 min at 37 °C, followed by a thorough washing with washing buffer. Then, 100 μL colorimetric solution A and B were

appended to the holes and incubated for 10 min at 37 °C, followed by addition of 50 μL stop solution.

3. Results and discussion

3.1. Principle of this method

The strategy is illustrated in Scheme 1. This DNA assembly include a aptamer DNA (1), a primer DNA (2), a protector DNA (3) and a template DNA (4). DNA (2) is composed of domains Ⅰ and Ⅱ. The domain Ⅰ is complementary to the domain Ⅰ′ of DNA (4) and the domain Ⅱ is complementary to the domain Ⅱ′ of aptamer DNA (1). Meanwhile, the DNA (3) of this assembly is composed of domains Ⅲ and Ⅳ which are complementary to the domains Ⅲ′ and Ⅳ′ of DNA (4). In the absence of the target for the aptamer, the aptamer DNA (1) prevents strand displacement reaction and extension reaction. The presence of the target, however, triggers release of the aptamer DNA from the DNA assembly, exposing the domain Ⅱ of DNA (2), leading to the displacement with DNA (3). The generation of DNA (2)/(4) complexes can trigger the polymerization reaction in the presence of polymerase and dNTPs. DsDNA structure with the recognition site for Nb.BbvCI then form

after polymerization reaction. After that, the 3′ end of the nicked strand triggers the next cycle of displacement, nicking and polymerization reaction. During this reaction, massive ssDNA (3) are regenerated. Then, toehold-mediated DNA strand displacement reactions between the DNA (3) and fluorescent/quencher labeled dsDNA (5)/(6) are performed. The increase of fluorescence provides an analytical signal. As shown in Fig. S1, the dabcyl functionalized DNA (6) was complementary with the FAM (Carboxy fluorescein) functionalized DNA (5), leaded to the quenching of fluorescent signal. Then, DNA (6) is displaced by DNA (3), resulting in an increase of fluorescent signal.

3.2. Characterization

The formation of DNA assembly was confirmed by an fluorescence experiment. The 5′ end of DNA (1), (2), (4) were functionalized with different fluorophores, respectively and the 3′ end of the DNA (2), (3), (4) were functionalized with quenchers. The four modified DNA named (1+), (2+), (3+) and (4+). As shown in Fig. 1A, the separation of the fluorophore and quencher ensured fluorescence intensity. On formation of the DNA assembly, the fluorophores and quenchers were co-localized on the same molecule, then fluorescence decrease. The results shown in Fig. 1B, the

fluorescent signals of DNA (1+); DNA (2+) and DNA (4+) were strong (red line) separately. When the four DNA mixed, the close proximity of all the fluorophores and quenchers made the fluorescence become very low (blue line).

This DNA assembly was also validated by a native polyacrylamide gel (PAGE) experiment. As shown in Fig. 1C, DNA assembly was effective synthesized without other heterochains (line 4). All these results confirmed the formation of the DNA assembly.

3.3. Feasibility analysis

Fig. 2A depicted that without target, aptamer DNA couldn't release from DNA assembly and then prevented the next reaction. While, the presence of the target, triggered release of the aptamer from the DNA assembly, exposed the domain Ⅱ of primer DNA (2), leaded to the displacement with DNA (3+) through a strand displacement process. After that, the unhybridized region of the DNA (3+) served as a toehold and complements with DNA (7), resulted in an decrease of fluorescence signal. The results were shown in Fig. 2B, fluorescence signal decreased quickly after DNA (2)(3+)(4) joined with DNA (7) (curve b), the result was the same as DNA (3+) joined with DNA (7) (curve a). The fluorescence signal decreased only because of dilution effect after DNA (1)(2)(3+)(4)

joined with DNA (7) (curve d), the result was the same as buffer solution join in DNA (7) (curve c). While, the fluorescence decreased gradually after $VEGF_{165}$ was added (curve d). The results showed that $VEGF_{165}$ can trigger structure switching of the DNA assembly and induce next reaction.

3.4. Optimization of complementary length

The presence of the target, however, triggers a structure-switching event that causes aptamer oligonucleotide competitive displaced from DNA assembly. Too strong binding force between aptamer DNA (1) and primer DNA (2) could prevent the displaced reaction. While, a weak binding force could also affect the stability of DNA assembly. Gibbs free energy ($\Delta G°$) of the combination of aptamer with target was calculated using the following equations:

$$\Delta G^0 = RTlnK_d$$

T is thermodynamics temperature (K), T = 310K. The dissociation constants (K_d) was calculated by using the data sets obtained from the SPR measurements, K_d = 1.4nM (Nonaka et al., 2010). R is a gas constant (8.314 J/mol·K). The calculation was ΔG^0 = -12.55 Kcal/mol. Withal, the $\Delta G°$ of different heteroduplex (1)/(2)

was evaluated through UNA fold software (http://mfold.rna.albany.edu/) to make a comparison (Table 1).

In order to investigate the optimum condition, three kinds of complementary lengths, whose $\Delta G°$ near to -12.55 Kcal/mol were selected to test. As shown in Fig. S2A, the aptamer labeled with Carboxytetramethylrhodamine (TAMRA) and the corresponding complementary base sequences modified with Dabcyl. Without the target for the aptamer, the fluorescence quenched. In the presence of the target, it triggered release of the aptamer from the dsDNA, leaded the rise of fluorescence signal. As the results shown in Fig. S2B, because of rich in GC base pairs, 10 complementary base pairs could prevent target binds with aptamer and 8 complementary base pairs accompanied with high background signal. Thus, 9 complementary base pairs were chosen as the optimum condition.

3.5. Optimization of the reaction temperature

The optimal reaction temperature of the proposed strategy was also investigated using the following experiments. As shown in Fig. 3A, quencher-modified DNA (6) and primer DNA (8) were complementary to fluorescence-labeled template DNA (9). The fluorescence signal was quenched in this nucleic acid structure. When the primer was extended by the DNA polymerase, the DNA

(7) released from this DNA structure caused an increase of fluorescent signal. The results shown in Fig. 3C, no fluorescence signal increase was observed without polymerase. In contrast, gradually increasing fluorescence signal was observed after polymerase added. The polymerase shown high efficiency at 37 °C and 45 °C. The ability of nicking enzyme Nb.BbvCI (5'-GC$^{\downarrow}$TGAGG-3') was confirmed by another experiment (Fig. 3B). Quencher-modified template DNA (10) was complete complementary to fluorescence-labeled DNA (9) and non-labeled DNA (3) was partial complementary to DNA (9). All the nucleic acids kept in the same concentration and the fluorescence signal was quenched at first. Then, this nucleic acid structure incubated with nicking enzyme at different temperature for 5 min. After that, upon heated to 95 °C, all duplexes were denatured. Whereafter, the temperature was reduced to 37 °C. If DNA (10) was nicked by nicking enzyme, the DNA (3) could bind with DNA (9) competitively, then resulted an increase of fluorescent signal. As the results shown in fig. 3D, when incubated with nicking enzyme at 37°C and 45°C for 5 min, the DNA (10) could be completely nicked. In conclusion, both polymerase and nicking enzyme had high efficiency at 37°C and 45°C. While, high temperature could lead to unstable of DNA assembly, and caused to a high background

signal (Fig. S3). So, 37 °C was chosen as the optimal reaction condition.

3.6. Analytical performance of the biosensor

Under the optimized conditions, the analytical performance of this method was evaluated by fluorescence real-time measurements. The fluorescence responses upon the target concentrations in the range from 0 pg/mL to 500 pg/mL were shown in Fig. 4A. The addition of target resulted in a signal increase compared with the blank (curve A). Fig. 4B illustrated the fluorescence signal increased linearly along with the increasing concentration of target DNA from 5 pg/mL to 400 pg/mL. The signal was slightly increased with the further increasing of target concentration, indicated a saturation condition, resulting from the competitive inhibition. The regression equation could be expressed as ΔF (a.u.) = 0.1976C (pg/mL) + 1.1281 with a correlation coefficient of 0.996, where ΔF was the fluorescence intensity variation and C was the concentration of target (n = 3). The limit of detection at a signal to noise ratio of 3 was calculated to be 3.5 pg/mL.

3.7. Specificity and repeatability of this sensing system

Due to the high affinity of aptamer to the target protein, the aptamer-based biosensors usually present excellent selectivity. In our investigation, SEB (staphylococcal enterotoxin B), LMP-1 (latent membrane protein), HE4 (human epididymis-specific protein 4) and PSA (prostate specific antigen) were used to perform control experiments to validate the specificity of the developed biosensor. As shown in Fig. S4, after the addition of equal concentrations of other kinds of proteins, low fluorescence signals were observed in contrast to the high response triggered by the target protein, which proved the high selectivity of the developed strategy. Thus, the non-target proteins could not cause the configuration change of the designed molecular beacon, leading no signal response. The error bars shown in Fig. S4 were obtained from three independent experiments respectively, also confirmed the high repeatability of the developed strategy.

3.8. Sample detection

To further test whether this strategy can be applied to $VEGF_{165}$ detection in real samples, five serum samples were collected from the first affiliated hospital, Chongqing medical university. 60 μL reaction system including 12 μL serum and the fluorescence signal interference from serum was low (Fig. S5). The detection results

were shown in Fig. 5A. The $VEGF_{165}$ concentration was calculated according to：

$$C\ (pg/mL) = \frac{5(\Delta F - 1.1281)}{0.1976} = 25.3\ \Delta F - 28.55$$

In order to evaluate the detectability of this method, a commercial ELISA kit was selected as control method (Fig. 5B). All the results were shown in Fig. 5C. The relevancy of the two methods was 0.9957 (Fig. 5D). Our developed aptamer-based sensor is regarded to be superior when compared with this antibody-based ELISA, because of its wider detection range, shorter detection time, easier operation and lower cost for test.

4. Conclusions

In summary, we have demonstrated a versatile amplified biosensing strategy that integrates structure switching aptamer for target recognition with both enzymatic isothermal amplification and toehold mediated DNA strand displacement reaction. The biosensor features a DNA assembly consists of a aptamer DNA, a primer DNA, a protector DNA and a template DNA. The target induced aptamer structure switching event acts as the control element for enzymatic isothermal amplification. A good linearity was obtained for $VEGF_{165}$ detection within the range of 5 pg/mL to 400 pg/mL

and a detection limit of 3.5 pg/mL. The performance of aptamer biosensor was successfully validated in serums and compared with conventional ELISA. Furthermore, our approach can also be potentially applied for diagnosis of other biomarkers of vital diseases.

Acknowledgments

This work was financially supported by Chongqing Yuzhong District Science and Technology Project (20140108), Chongqing Medical Scientific Research Projects (20142167) and Natural Science Foudation of Inner Mongolia (2015MS0850).

References

Abdel-Rahman, O., 2015. Crit. Rev. Oncol. Hemat. 93(1), 18-27.

Belcik, J.T., Qi, Y., Kaufmann, B.A., Xie, A., Bullens, S., Morgan, T.K., Bagby, S.P., Kolumam, G., Kowalski, J., Oyer, J.A., Bunting, S., Lindner, J.R., 2012. J. Am. Coll. Cardiol. 60(7), 618-625.

Chen, H., Hou, Y., Qi, F., Zhang, J., Koh, K., Shen, Z., Li, G., 2014. Biosens. Bioelectron. 61, 83-87.

Cho, H., Yeh, E.C., Sinha, R., Laurence, T.A., Bearinger, J.P., Lee, L.P., 2012. ACS Nano 6, 7607-7614.

Do, D.V., Nguyen, Q.D., Vitti, R., Berliner, A.J., Gibson, A., Saroj, N., Soo, Y., Boyer, D.S., 2016. Ophthalmology 123(4), 850-857.

Domigan, C.K., Ziyad, S., Arispe, M.L.I., 2015. Arterioscler. Thromb. Vasc. Biol. 35, 30-39.

Freeman, R., Girsh, J., Jou, A.F., Ho, J.A., Hug, T., Dernedde, J., Willner, I., 2012. Anal. Chem. 84(14), 6192-6198.

Gao, L., Li, Q., Li, R., Yan, L., Zhou, Y., Chen, K., Shi, H., 2015. Nanoscale 7(25), 10903-10907.

Goncalves, V., Gautier, B., Garbay, C., Vidal, M., Inguimbert, N., 2007. Anal. Biochem. 366(1), 108-110.

Gupta, N., Mansoor, S., Sharma, A., Sapkal, A., Sheth, J., Falatoonzadeh, P., Kuppermann, B.D., Kenney, M.C., 2013. The Open Ophthalmology Journal 7, 4-10.

Guo, Y., Wu, J., Ju, H., 2015. Chem. Sci. 6(7), 4318-4323.

Jeong, J.-E., Kim, B., Woo, S., Hwang, S., Bazan, G.C., Woo, H.Y., 2015. Chem. Sci. 6(3), 1887-1894.

Kirsch, J., Siltanen, C., Zhou, Q., Revzin, A., Simonian, A., 2013. Chem. Soc. Rev. 42(22), 8733-8768.

Kwon, O.S., Park, S.J., Jang, J., 2010. Biomaterials 31(17), 4740-4747.

Kwon, O.S., Park, S.J., Hong, J.Y., Han, A.R., Lee, J.S., Lee, J.S., Oh, J.H., Jang, J., 2012. ACS Nano 6, 1486-1493.

Lee, S.E., Chen, Q., Bhat, R., Petkiewicz, S., Smith, J.M., Ferry, V.E., Correia, A.L., Alivisatos, A.P., Bissell, M.J., 2015. Nano letters 15(7), 4564-4570.

Leung, D.W., Cachianes, G., Kuang, W.J., Goeddel, D.V., Ferrara, N., 1989. Science 246, 1306-1309.

Li, C., Li, X., Wei, L., Liu, M., Chen, Y., Li, G., 2015a. Chem. Sci. 6(7), 4311-4317.

Li, J., Chen, Z., Xiang, Y., Zhou, L., Wang, T., Zhang, Z., Sun, K., Yin, D., Li, Y., Xie, G., 2016. Biosens. bioelectron. 86, 75-82.

Li, W., Zhang, Q., Zhou, H., Chen, J., Li, Y., Zhang, C., Yu, C., 2015b. Anal. Chem. 87(16), 8336-8341.

Liu, M., Zhang, W., Zhang, Q., Brennan, J.D., Li, Y., 2015. Angew. Chem. 54(33), 9637-9641.

Marone, G., Varricchi, G., Loffredo, S., Granata, F., 2016. Eur. J. Pharmacol. 778, 146-151.

Nie, J., Zhao, M.-Z., Xie, W.J., Cai, L.-Y., Zhou, Y.-L., Zhang, X.-X., 2015. Chem. Sci. 6(2), 1225-1229.

Niu, G., Chen, X., 2010. Curr. Drug Targets 11, 1000-1017.

Nonaka, Y., Sode, K., Ikebukuro, K., 2010. Molecules 15(1), 215-225.

Nonaka, Y., Yoshida, W., Abe, K., Ferri, S., Schulze, H., Bachmann, T.T., Ikebukuro, K., 2013. Anal. Chem. 85(2), 1132-1137.

Park, M.S., Kim, B.R., Dong, S.M., Lee, S.H., Kim, D.Y., Rho, S.B. Oncotarget 2014, 5, 4935-4944.

Potyrailo, R.A., Murray, A.J., Nagraj, N., Pris, A.D., Ashe, J.M., Todorovic, M., 2015. Angew. Chem. 54(7), 2174-2178.

Prior, S.J., Hagberg, J.M., Paton, C.M., Douglass, L.W., Brown, M.D., McLenithan, J.C., Roth, S.M., 2006. Am. J. Physiol-Heart C. 290, 1848-1855.

Rifai, N., Gillette, M.A., Carr, S.A., 2006. Nat. Biotechnol. 24(8), 971-983.

Senger, D.R., Galli, S.J., Dvorak, A.M., Perruzzi, C.A., Harvey, V.S., Dvorak, H.F., 1983. Science 219, 983-985.

Takahashi, H., Nomura, Y., Nishida, J., Fujino, Y., Yanagi, Y., Kawashima, H., 2016. Invest. Ophthalmol. Vis. Sci. 57(2), 462-466.

Tsai, M.J., Wang, T.N., Lin, Y.S., Kuo, P.L., Hsu, Y.L., Huang, M.S., 2015. J. Mol. Med. 93(11), 1257-1269.

Urquidi, V., Goodison, S., Kim, J., Chang, M., Dai, Y., Rosser, C.J., 2012. Urology 79(5), 1185 e1181-1186.

Van Ness, J., Van Ness, L.K., Galas, D.J., 2003. P. Natl. Acad. Sci. USA. 100(8), 4504-4509.

Wang, S.E., Si, S., 2013. Appl. Spectrosc. 67(11), 1270-1274.

Wei, K., Piecewicz, S.M., McGinnis, L.M., Taniguchi, C.M., Wiegand, S.J., Anderson, K., Chan, C.W., Mulligan, K.X., Kuo, D., Yuan, J.,

Vallon, M., Morton, L.C., Lefai, E., Simon, M.C., Maher, J.J., Mithieux, G., Rajas, F., Annes, J.P., McGuinness, O.P., Thurston, G., Giaccia, A.J., Kuo, C.J., 2013. Nat. Med. 19(10), 1331-1337.

Wimmer, T., Lorenz, B., Stieger, K., 2016. Biosens. Bioelectron. 86, 609-615.

Xue, L., Qiu, H., Li, Y., Lu, L., Huang, X., Qu, Y., 2011. Colloid Surf. B 82(2), 432-437.

Zhang, H., Li, M., Li, C., Guo, Z., Dong, H., Wu, P., Cai, C., 2015. Biosens. Bioelectron. 74, 98-103.

Zhao, S., Ma, W., Xu, L., Wu, X., Kuang, H., Wang, L., Xu, C., 2015a. Biosens. Bioelectron. 68, 593-597.

Zhao, Y., Chen, F., Li, Q., Wang, L., Fan, C., 2015b. Chem. Rev. 115(22), 12491-12545.

Scheme 1. The principle of the fluorescence biosensor for VEGF detection.

Fig. 1. (A) DNA modified with fluorophores and quenchers. (B) Fluorescence intensities of DNA (4+), (2+), (1+), respectively (red line); Fluorescence intensities of DNA assembly (blue line). (C) Gel

electrophoresis. lane 1: 20 bp DNA Ladder; lane 2: DNA (1)(2); lane 3: DNA (3)(4); lane 4: DNA (1)(2)(3)(4).

Fig. 2. (A) Schematic illustration of feasibility analysis. (B) lane a: 50 μL DNA (7) + 50 μL DNA (3+) at 1 min; lane b: 50 μL DNA (7) + 50 μL DNA (2)(3+)(4) at 1 min; lane c: 50 μL DNA (7) + 50 μL Buffer at 1 min; lane d: 50 μL DNA (7) + 50 μL DNA (1)(2) (3+)(4) at 1 min + 2 μL, 800 ng/mL $VEGF_{165}$ at 5 min. All the DNA concentration was 200 nM.

Fig. 3. (A) Schematic diagram of the polymerase efficiency verification. (B) Schematic diagram of the nicking enzyme efficiency verification. (C) Real-time monitoring of the fluorescence signal under enzymatic polymerization at different temperatures. (D) Fluorescence intensities of enzymatic nicking at different temperatures.

Fig. 4. (A) Real-time fluorescence signals with the increasing concentrations of target (from 0, 5, 20, 100, 200, 300, 400, 500 pg/mL, respectively). (B) Calibration curve of the fluorescence signal variation versus the target concentration.

Fig. 5. (A) Time-dependent fluorescence response of biosensor for $VEGF_{165}$ from clinical samples. (B) ELISA for $VEGF_{165}$ from clinical

samples. (C) The detection results of aptamer biosensor and ELISA methods. (D) The relevancy of aptamer biosensor and ELISA detection results.

Table 1 Thermodynamic parameters evaluated by software

Name	Complementary length	*T (K)*	*ΔH°* (Kcal/mol)	*ΔS°* (cal/mol/K)	*ΔG°* (Kcal/mol)
	7	310	-102.1	-300.0	-9.1
DNA(10)	8	310	-110.1	-319.2	-11.1
DNA (11)	9	310	-68.4	-181.1	-12.2
	10	310	-118.2	-335.5	-14.1
DNA (12)	11	310	-91.6	-243.5	-16.1

Highlights

- We have demonstrated a versatile aptasensor strategy based on enzymatic isothermal amplification to signal enlargement.
- A low target content could be detect due to the isothermal amplification process.
- The proposed strategy could be extended to the detection of other targets by simply exchanging the corresponding aptamer sequence.